Chemical Engineering Journal 154 (2009) 315–324

Contents lists available at ScienceDirect

Chemical Engineering Journal

journal homepage: www.elsevier.com/locate/cej

Combustion of methane–hydrogen mixtures on catalytic tablets

Andrea Scarpa[a], Paola Sabrina Barbato[a], Gianluca Landi[b], Raffaele Pirone[b,*], Gennaro Russo[a]

[a] Dipartimento di ingegneria chimica, Università degli Studi "Federico II" di Napoli, p.le Tecchio 80, 80125 Napoli, Italy
[b] Istituto di Ricerche sulla Combustione, CNR, p.le Tecchio 80, 80125 Napoli, Italy

ARTICLE INFO

Article history:
Received 11 January 2009
Received in revised form 1 April 2009
Accepted 11 May 2009

Keywords:
Micro-combustor
Methane
Hydrogen
Catalysis

ABSTRACT

Catalytic micro-combustors have been developed via deposition of active layers of Pt/γ-Al_2O_3, $LaMnO_3$/γ-Al_2O_3 and Pt-$LaMnO_3$/γ-Al_2O_3 on FeCralloy and α-Al_2O_3 slabs. Diffusional resistance in the gas phase have been experimental excluded, even if catalyst is present on only one side of the reactor. Pt/γ-Al_2O_3 gave best performances in the combustion of H_2 while $LaMnO_3$/γ-Al_2O_3 revealed to be the best catalyst for methane combustion. The mixture Pt–$LaMnO_3$ supported on γ-Al_2O_3 showed intermediate properties for both fuels.

The combustion of H_2–CH_4 mixtures showed that the presence of hydrogen promotes the oxidation of methane, since above 700 °C radical reactions involving CH_4 are activated by H_2 ignition.

1. Introduction

Despite their large use, the low energy density of conventional batteries is a limit for the miniaturization and portability of a lot of electronic devices of common use [1]. On the other hand, any fossil fuel shows an energy density at least 50 times higher than a typical Li battery, so rendering the development of alternative processes of in situ generation of electricity via fuel combustion a very intriguing innovation for portable applications. Moreover, practical considerations related to fast and simple recharge and low cost of liquid fuels render the required efficiency for such novel processes not extremely high (i.e. 1–5%) to be successful. However, such a new technique must need effective and relatively integrated conversion systems to transform energy from thermal to electrical power. Several power generators have been proposed for converting combustion heat into electricity [2–5]. Among these, interest exists in direct conversion systems, such as thermoelectrics (TE) and thermo-photovoltaics (TPV), due to the absence of moving parts [3,6]. However, even if TE or TPV elements need relatively high temperature to work efficiently, a high durability is exhibited provided temperature does not exceed 800 °C or even much lower in the case of thermoelectric conversion systems, for most commercial materials up to date developed.

Such temperatures are too low for a homogeneous combustion flame to be sustained, especially considering that the scales of interest in the field of the MEMS (1000–100 μm) approach the quenching distance for most possible fuels; so the application of a catalytic system appears the most attractive option, if not the unavoidable one. Actually, the use of a catalyst should guarantee a stable exercise of the process even in strongly diluted conditions, allowing a very uniform thermal profile too, with consequent improvements of conversion system efficiency.

Micro-scale catalytic combustion has been receiving a lot of attention. In most cases, ceramic flat substrates supporting noble metals based catalysts have been investigated, mainly in the combustion of hydrogen or very volatile liquid hydrocarbons, such as propane and butane [7–9]. High volatility and low chemical and thermal stability [10–12] does not render noble metal catalysts very suitable for high temperature applications driving the research interests towards less expensive transition metal mixed oxide based catalysts [13].

Despite its large diffusion, availability and consolidated distribution systems, few attentions have been devoted to the combustion of methane, whose low reactivity requires higher temperatures for the complete conversion. On the other hand, methane is the cleanest fuel with the highest H/C ratio amongst hydrocarbons and should be seen as the desirable fuel for residential applications. The use of pure H_2 is very interesting too. Hydrogen is now seen as the optimal energy vector, especially as produced by alternative energy sources other than fossil fuels. It can generate energy with virtually zero emission, even if the problems of its production, storage and transportations do not appear close to a satisfactorily solution yet.

On the other hand, particular attention has been recently devoted to the study of the hydrogen–methane mixture providing high methane combustion rate, notwithstanding its relatively low reactivity (compared to other hydrocarbons), and high H/C ratio with favourable consequence on global warming, both in homogeneous flames and catalytic reactors [14–17]. Use of such mixtures could be seen as the first tool for hydrogen to penetrate the energy market (mixtures with methane will overcome most

* Corresponding author. Tel.: +39 0817682235; fax: +39 0815936936.
E-mail address: pirone@irc.cnr.it (R. Pirone).

1385-8947/$ – see front matter © 2009 Elsevier B.V. All rights reserved.
doi:10.1016/j.cej.2009.05.013

of the problems of transportation and storage), as well as the mean of better burning CH_4, if the higher reactivity of hydrogen will help the combustion of methane too. Hydrogen addition to the fuel enhances homogeneous methane reaction [16–18] by producing more H, O and OH radicals. On the contrary, H_2 reaction rate resulted depleted, probably due to a competitive mechanism between reaction steps involving the same radicals. Moreover, the modifications of the reaction rates appeared related to H_2/CH_4 and equivalence ratios, lean mixtures showing the most significant increase of the CH_4 burning velocity.

In this work, we have investigated the properties of a series of catalysts obtained from inert substrates in the shape of plates of two different materials characterized by variable thermo-conductibility (α-Al_2O_3, FeCralloy), that have been coated with a γ-Al_2O_3 washcoat and a perovskite-type active phase constituted by $LaMnO_3$ (supported onto alumina pores). The effect of doping perovskite with a little amount of platinum has been taken into account too and, thus, Pt/Al_2O_3 catalyst has been also prepared and tested as reference material. Methane, hydrogen and their mixtures have been used as gaseous fuels.

2. Experimental

2.1. Catalysts preparation

Catalysts have been preliminarily prepared in form of powders by supporting on γ-Al_2O_3 the active phases alternatively constituted by Pt, $LaMnO_3$ and Pt–$LaMnO_3$. γ-Alumina powder (CK300, Akzo) is finely grounded by means of a "ball milling" machine till the mean diameter of the particles is less than 2 μm. In order to prevent γ- to α-alumina transition at high temperatures, lanthanum oxide (5 wt%) is inserted into the structure as stabilizer [19]. After this operation, the active phase is loaded up.

The active phase and La_2O_3 are deposed through an "incipient wetness impregnation" method in a rotary vapour (Laborota 4002, Heidolph). According to this method the inert alumina powder is suspended in an aqueous solution constituted by the precursor salts of stabilizer or active phase. The precursor salts are added to the solution in such an amount to have the desired load and formulation of the catalysts. The prepared suspension is fed into the rotary vapour rotating at 75 rpm and it is dried under vacuum conditions (100 mbar) at 50 °C. The dried impregnated powder is consequently calcined at 800 °C for 3 h in air. In the case of Pt/γ-Al_2O_3 samples, an impregnation solution constituted by a diluted chloroplatinic acid solution (Sigma–Aldrich) has been prepared, while manganese acetate (Manganese acetate tetrahydrate, Aldrich) and lanthanum nitrate (Lanthanum nitrate Hexahydrate, Fluka) has been used in the case of $LaMnO_3/\gamma$-Al_2O_3 based catalyst. Finally, in the case of the Pt–$LaMnO_3/\gamma$-Al_2O_3 catalysts, a solution constituted at the same time by the precursors of Pt, Mn and La has been involved.

Alumina platelets, characterized by an elevated thermal, mechanical and chemical resistance, have been prepared starting from precursors supplied by Cotronics Corp. According to the recipe supplied by Cotronics [20], a specific amount of alumina powder (Rescor 780) and a liquid activator (Rescor 780 Activator), which generates intra-particle reactions favouring to the formation of a unique alumina block, are poured in a beaker and properly mixed until obtaining a slurry provided with a certain consistency. The slurry is then poured in the formerly prepared mould. The platelets are prepared in the required shape and dimensions through the use of specific home-made flexible and impermeable moulds, 0.5 cm thick, 1.5 cm wide and 3.0 cm long. The slurry inside the mould is dried at room temperature for about 20 h. After such operation the mechanical resistance is high enough to allow the removal of the platelet from the mould and the sample is further heated up to 950 °C (1 °C/min) for 5 h. Such thermal treatment determines a further increase in the mechanical resistance as well as the removal of the organic part present in the liquid activator.

FeCralloy based samples have been prepared from foils (Good Fellow), which thickness is 2 or 5 mm, that are properly cut in order to obtain 1.5 cm wide and 3.0 cm long samples. The substrates undergo to a specific thermal treatment in air whose aim is the growth of γ-alumina layer in the form of whiskers on the surface [21]. These structures, interposing between the FeCralloy surface and the catalytic layer, improve the anchoring because of their greater chemical affinity with the deposed film respect to the metallic substrate.

In order to deposit the catalytic film on the FeCralloy and alumina substrates, a "slurry" constituted by the fresh powder catalysts is prepared. Powders are mixed with Boehmite (Disperal, Sasol), used as binder. The solid mixture is thus suspended in an aqueous solution of nitric acid. The slurry is spread on the plates through a paintbrush and is subsequently dried at 120 °C for 20 min. It is, finally, calcined at 800 °C for 3 h, in order to anchor the catalytic film on the substrate. A picture of substrates and so prepared catalysts is reported in Fig. 1.

Moreover, the slurry used in the preparation of the catalytic platelets is further calcined; the resulting powder catalyst is used as reference in the kinetic measurements in order to evaluate the effectiveness of the deposition technique.

Nomenclature and some detail of catalysts prepared are reported in Table 1, where the samples are labelled according to substrate material (F: FeCralloy, A: α-alumina), slab height (2 or 5 mm) and active phase supported on the washcoat constituted by the LaO-stabilised γ-Al_2O_3 layer (LM: perovskite; Pt1: Pt 1 wt%). Table 1 also reports the amount of the catalytic layer loaded and the nominal percentages of active components for the samples investigated. The sample A5 is a blank platelet made of α-Al_2O_3 and finally PwLM is the powder sample obtained by calcining the slurry employed to prepare perovskite supported structured catalysts. All catalysts are subjected to an ageing treatment at 800 °C in air lasting maximum 30 h before being tested.

Chemical composition of the washcoat has been measured by means of inductively coupled plasma (ICP) analysis, performed on an Agilent 7500 ICP-MS instrument, while the adhesion of the active layer has been tested by ultrasound treatment (30 min) in a ultrasonic bath (Quantex 90H, L&R Manufacturing) in order to evaluate the resistance to mechanical stresses.

2.2. Combustion tests

Activity tests have been carried out under isothermal and strongly diluted conditions. In such conditions the power generated

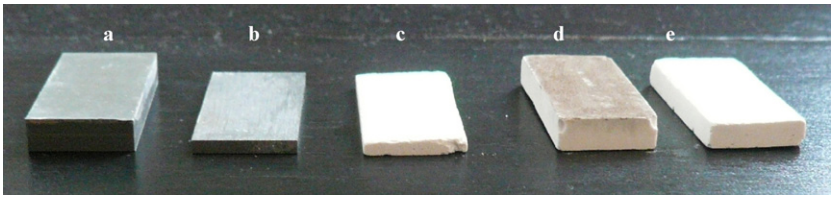

Fig. 1. Uncoated substrates: FeCralloy 2 mm high (b), α-Al_2O_3 2 mm high (c) and 5 mm high (e); and washcoated catalysts: FeCralloy 5 mm high (a), α-Al_2O_3 5 mm high (d).

Table 1
Catalysts prepared for the present study: code, substrate material, amount of catalytic layer loaded on the slab, nominal loading of active components and height of platelets.

Code	Substrate	Amount of catalyst mg	Active phase loading, %		Height, mm	
			$LaMnO_3$	Pt	plate	gap
F5LM	FeCralloy	16	20	–	5	1
F5Pt1LM	FeCralloy	17	20	1	5	1
F5Pt1	FeCralloy	17	0	1	5	1
F2LM	FeCralloy	14	20	0	2	4
A5LM	Alumina	19	20	0	5	1
A5Pt1LM	Alumina	32	20	1	5	1
A5	Alumina	0	0	0	5	1
PwLM	Powders	–	20 (18.5)	0	–	–

by the reaction is not enough to guarantee auto-thermal process and an external power source is needed to carry out the reaction. On the contrary, the amount of heat released by the conversion of fuel is almost negligible with respect to the warming power exchanged, so that isothermal and controlled conditions could be assured. An electric oven is employed to heat the catalytic combustor until a specific reaction temperature. Specifically, activity tests have been performed at a maximum temperature equal to 800 °C.

Hydrogen and methane oxidation tests have been carried out at different flow rates in the range 15–70 standard litres per hour (slph). Fuel percentage in the mixture was 0.25 vol% in the case of methane and 1 vol% in the case of hydrogen (in both the cases fuel concentration is below the lower flammability limit (LFL) that is 4% and 5%, respectively for H_2 and CH_4), thus approximately supplying the same overall heating value of 80 J Nl^{-1} despite of the fuel. Oxygen content is four times higher than the stoichiometric value required for complete combustion occurrence, corresponding to an equivalence ratio (Φ) equal to 0.25. In the following, kinetic constant for H_2 and CH_4 combustion will be calculated according to plug flow reactor (PFR), first order kinetic with respect to the fuel and zero order with respect to oxygen assumptions. For the combustion of H_2–CH_4 mixtures, experiments have been carried out by varying the H_2/CH_4 ratio at a total flow rate varying between 15 and 70 slph. As reported in Table 2, Mix1 up to Mix6 are characterized by a growing content of H_2 while leaving the overall calorific value of the fuel approximately constant (80 J Nl^{-1}). The molar fuel fraction of hydrogen in the H_2–CH_4 mixtures varies from 0% in Mix1 to 91% in Mix6, corresponding to a maximum energetic substitution equal to 75% of the total power input.

Catalysts have been inserted in a stainless steel (AISI 310S) reactor (SSR), suitable for high temperature operation, provided with a cavity (1.5 cm × 0.6 cm × 3.0 cm) that allows the precise placement of the platelets and leaves an open volume above it for gas flow. An overall drawing and an explosion view of the reactor are reported in Fig. 2a and b; SSR is constituted by a flanged block where the platelet is placed in the cavity described above between two SiC foam acting as flow distributors. Another flange is used as cover and a metallo-plastic gasket, inserted between the flange and the flanged block, avoids gas leaks. In this configuration the gaseous mixture flows from one side to the other passing in the distributor upstream to the catalyst, over the platelet and in the second distributor (Fig. 2c). Several holes made in the upper and bottom zones allows thermocouples insertion and temperature profile measurements.

The strong diluted conditions adopted guarantee an isothermal profile along the reactor despite of the combustion heat, as we have carefully measured with a set of thermocouples placed along the reactor.

Table 2
Hydrogen substitution and operating conditions considered in H_2–CH_4 mixtures combustion tests.

	Molar composition			H_2 in H_2–CH_4, %	
	CH_4, %	H_2, %	H_2/CH_4 ratio	Molar	Energetic
Mix 1	0.25	0	0	0	0
Mix 2	0.21	0.21	1.0	50	23
Mix 3	0.17	0.34	2.0	67	38
Mix 4	0.14	0.46	3.3	77	50
Mix 5	0.11	0.55	5.0	83	60
Mix 6	0.07	0.68	10.0	91	75
Mix 7	0	0.34	–	100	100
Mix 8	0	0.46	–	100	100
Total flow rate = 15/70 slph					

3. Results

ICP analysis revealed that both fresh and supported powder catalysts show composition close to the theoretical one.

The good adhesion of the catalytic layer has been tested under thermal and mechanical stresses. At this proposal, the catalytic substrates have been subjected to mechanical stresses at room temperature in an ultrasonic bath showing a weight loss lower than 5 wt% of the sole layer. Moreover, thermal stresses obtained through several ageing cycles performed in air at 800 °C progressively up to a maximum time length of 30 h showed that a weak de-activation of the catalyst was observed in the first 12 h of ageing, but after longer treatments the decreasing in fuel conversion is no more significant. It follows that a 12 h treatment is long enough to obtain a catalytic system working in stable conditions and assure that high temperature operation does not involve a worsening in catalyst performances due to chemical and physical deactivation phenomena (sintering, solid–solid interactions [22–24]).

Fluid dynamic issues are particularly relevant in structured catalytic reactors, and in particular in a micro-combustor. Gas bypassing, channelling and the presence of dead volumes must be avoided in order to obtain high combustor efficiency. Moreover, fuel conversion may be transport-limited thus preventing an efficient use of the catalyst, especially in a fully developed laminar flow, typical in micro-combustion applications. SiC foams inserted before and after the catalytic plates are determinant in minimizing flow bad-distribution (gas channelling and stagnation).

Fluid dynamic features of the reactor have been theoretically and experimentally studied. In the experimental conditions investigated, Re number varies between 20 and 60. At the entrance section the velocity profile is flat and the length required to allow the full development of the laminar regime can be calculated according the Eq. (1), under the hypothesis of isothermal and incompressible flow [25].

$$L_{ent} = 0.035\delta_H Re \leq 4\,\text{mm} \quad (1)$$

where δ_H is the equivalent diameter of the reactor (=0.002 m) corresponding to less than 10% of the overall length of the reactor. As a consequence, the flow through the reactor can be well approximated as fully developed laminar. In these conditions a Sh number equal to 4 can be considered [26], corresponding to a diffusion velocity $K_D = 0.41\ m\ s^{-1}$. Using the values reported above, the Peclet number results equal to about 30, a value enough high to consider

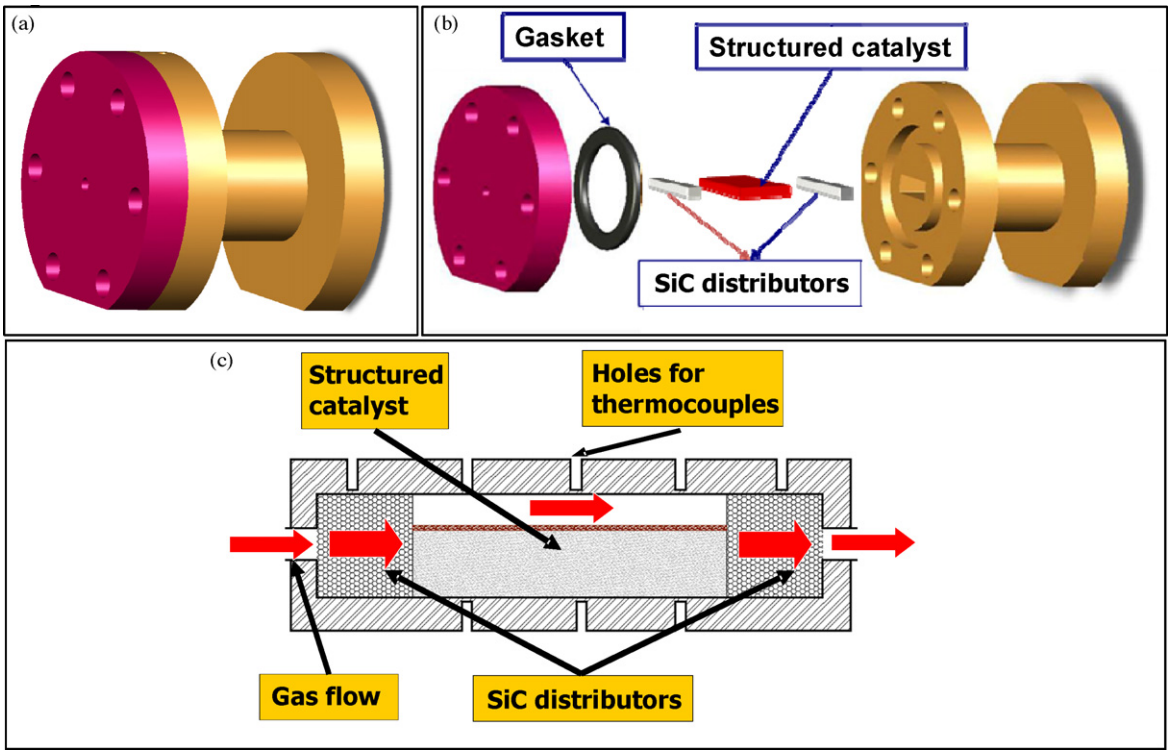

Fig. 2. Drawings of the stainless steel reactor (SSR): (a) overall view; (b) explosion view; (c) section and gas pathway.

the reactants diffusion on the catalytic substrate satisfactorily efficient to avoid gas exiting from the reactor without contacting the catalyst.

On the other hand the relative importance between mass transfer and intrinsic surface kinetics has been experimentally investigated. Specific tests have been conducted at fixed flow rate changing the height of the chamber (so changing the residence time τ_R, defined as the ratio between the void volume present above the slab and the gas flow rate) by varying the height of the substrate platelet, but not the catalyst amount (thus keeping constant the contact time τ_C, defined as the ratio between the mass of catalyst loaded and the gas flow rate). In particular, reaction tests have been performed at 40 slph increasing the channel gap from 1 to 4 mm. F2LM catalytic platelet has been involved for such an analysis, which is 2 mm thick, so providing a combustion (void) chamber 4 mm high. In order to change the height of the channel some wedges are inserted below the catalytic slab to increase the overall platelet thickness up to 5 mm and consequently reducing the height of the void volume down to 1 mm.

Fig. 3a shows the results of such tests by reporting CH_4 conversion as a function of the reactor temperature. It seems evident that methane conversion is not affected by the height of the combustion chamber, since the differences measured among conversion data lie within the experimental noise, suggesting the absence of any transport limitation on fuel catalytic conversion. On the other hand, the results reported in Fig. 3b show that the kinetic constant

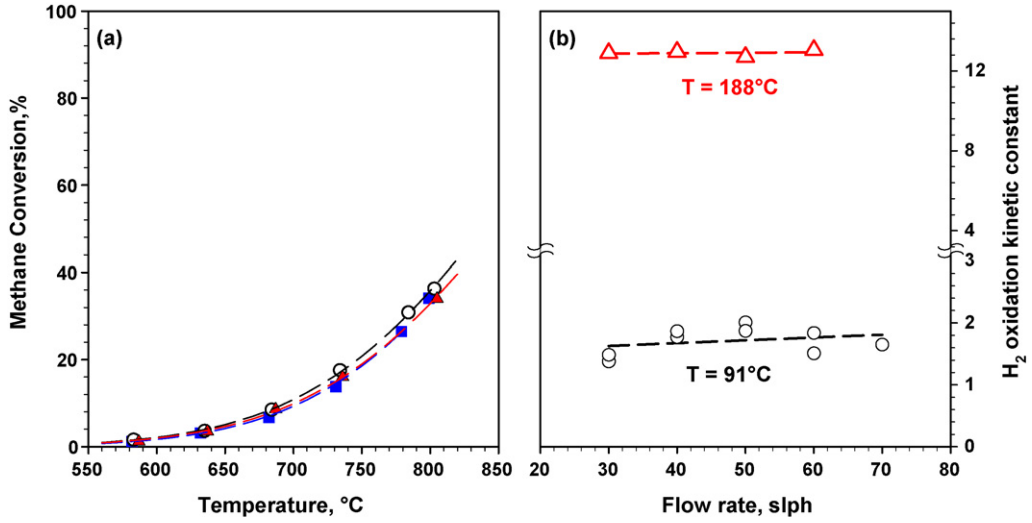

Fig. 3. Combustion tests on Fe_2LM in SSR: (a) CH_4 conversion as a function of temperature at $\tau_C = 1.26\ g_{cat}\ s\ Nl^{-1}$ and 0.25% inlet concentration of methane with variable combustion chamber height (δ): $\delta = 4$ mm (▲); $\delta = 3$ mm (○); $\delta = 1$ mm (■); (b) kinetic constant of H_2 oxidation as a function of the flow rate, evaluated under the hypotheses of plug flow reactor and first order rate expression at 1% inlet concentration of hydrogen.

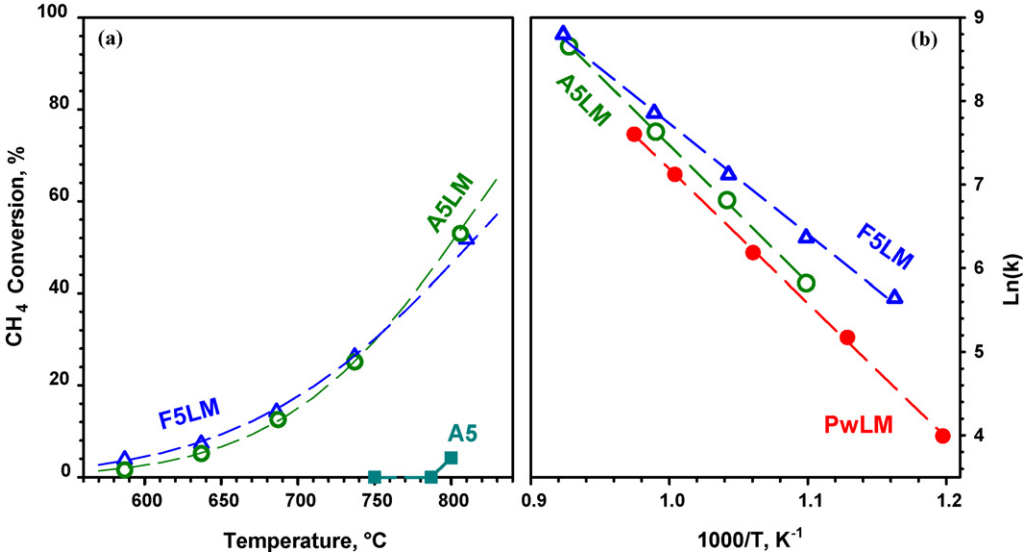

Fig. 4. Effect of the substrate on the catalytic activity in CH_4 combustion of perovskite based systems: (a) CH_4 conversion as a function of the temperature; (b) Arrhenius plot. Catalysts: F5LM (Δ), A5LM (○), A5 (■) and PwLM (●).

for H_2 oxidation estimated under the hypotheses of plug flow reactor and first order rate equation is not significantly variable with the flow rate, witnessing no diffusion effect on hydrogen conversion in the experimental conditions explored.

A possible effect of the substrate on catalytic performance has been studied by carrying out tests of CH_4 combustion over $LaMnO_3/Al_2O_3$ based catalyst deposited on slab-shaped substrates of different materials (A5LM vs. F5LM). Moreover, powder catalyst (PwLM) and an inert alumina slab (A5), free of active phase, have been also tested as references respectively for intrinsic kinetics and gas phase reactions contribution. The experiments have been performed in a 1 mm high combustion chamber at a total flow rate equal to 40 slph.

Results of methane combustion are reported in Fig. 4a and b (Arrhenius plots) and in Table 3. The activity of F5LM and A5LM catalytically coated slabs of different materials are very similar, suggesting that the interaction with the substrates does not significantly alter the active phase. CH_4 conversion detected at the maximum temperature is limited to about 50% on both structured catalysts. However, F5LM sample seems to result somewhat more active at low temperature, probably to its higher thermal conductivity. This results in a lower activation energy (26.2 kcal mol^{-1} vs. 32.6 kcal mol^{-1}), as calculated by the Arrhenius plots reported in Fig. 4b. In Fig. 4a the performance of A5 is also reported; maximum CH_4 conversion is around 5%, much lower than that provided by the catalytic platelets, strongly evidencing the insignificant role of gas phase reaction pathways.

The performance of powder catalyst has not been reported in Fig. 4a due to the different contact times employed, allowing only the comparison among Arrhenius plots showed in Fig. 4b. Comparing the kinetic data of PwLM with those of A5LM, it results a slightly lower kinetic constant evaluated at 800 °C while approximately the same activation energy. On the basis of these results, the characteristic feature of the kinetics of the methane oxidation on perovskite based catalysts seems to be unchanging by passing from a powder to a structured material, as it is attested by the same value measured for the activation energy. On the contrary, by depositing the catalyst on a substrate a better dispersion is achieved thus allowing an increase in the number of the active sites available for the reaction to occur, as suggested by the increase in the pre-exponential factor of the kinetic constant estimated. Comparing the performances of PwLM with those of FeCralloy catalytic substrates, the previous considerations are still valid. Nevertheless, an increase in perovskite activity is observed in the case of F5LM while it is not significant for F2LM (not reported). This is due to a better dispersion obtained on the F5LM sample related to the amount of the "taken out" γ-alumina, greater and greater with increasing the thickness of the substrate.

Different γ-alumina supported active phases have been tested in methane combustion. In particular, perovskite, platinum and the phase constituted by their mixture are taken into account with the aim of studying the effect of the co-presence of platinum and perovskite in the active phase on the measured combustion rate. The activity of F5LM is compared with that of F5Pt1LM and F5Pt1, tested under the same operating conditions. The results are shown in Fig. 5, in terms of fuel conversion and selectivity to CO as functions of temperature, while in Table 4 the estimated kinetic parameters are reported. It is worth noting that the presence of CO among by-products is a signal of the occurrence of homogeneous reaction paths (of methane oxidation to CO and H_2O), that in such a range of temperature and residence time cannot succeed in converting fuel towards the deepest oxidation product CO_2.

Comparing the performances of F5LM and F5Pt1LM, it is clearly shown that the addition of platinum to the γ-alumina supported perovskite is not effective in enhancing catalytic performances. On the contrary, the co-presence of Pt and perovskite gives rise to a worsening of the unpromoted $LaMnO_3/\gamma\text{-}Al_2O_3$ sample, as

Table 3
Effect of the substrate material on the perovskite catalytic activity in CH_4 combustion.

Catalyst code	τ_C, g_{cat} s Nl^{-1}	E, Kcal mol^{-1}	k_0, Nl s^{-1} $g_{cat}{}^{-1}$	k (800 °C), mmol s^{-1} $g_{cat}{}^{-1}$
F5LM	1.44	26.2	3.6×10^5	18.0
A5LM	1.71	32.6	7.0×10^6	17.0
PwLM	18.0	31.8	3.5×10^6	12.0

Table 4
Effect of the active phase on CH_4 combustion.

Catalyst code	τ_C, g_{cat} s Nl^{-1}	E, Kcal mol^{-1}	k_0, Nl s^{-1} $g_{cat}{}^{-1}$	k (800 °C), mmol s^{-1} $g_{cat}{}^{-1}$
F5LM	1.44	26.2	3.6×10^5	18.0
F5Pt1LM	1.53	29.0	1.1×10^6	15.0
F5Pt1	1.49	27.7	3.3×10^5	8.0

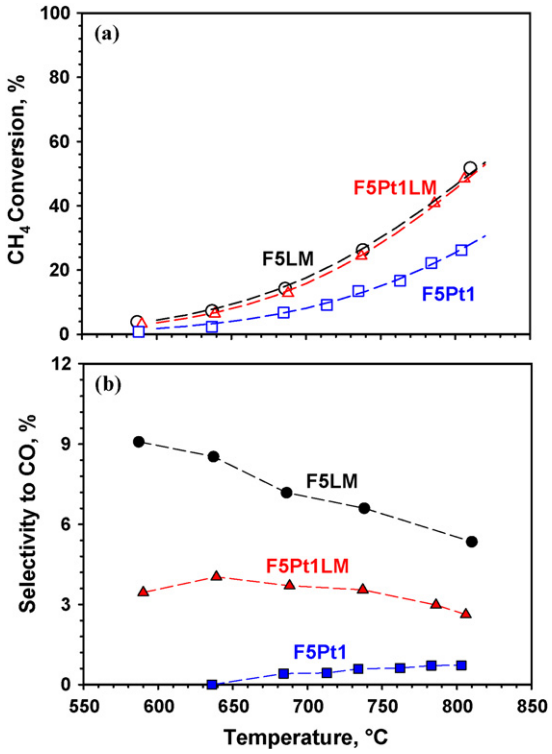

Fig. 5. Methane combustion on different catalysts. (a) Fuel conversion as a function of the temperature; (b) selectivity to CO. F5LM, $\tau_C = 1.44\ g_{cat}\ s\ Nl^{-1}$ (○, ●); F5Pt1LM, $\tau_C = 1.53\ g_{cat}\ s\ Nl^{-1}$ (▲, △); F5Pt1, $\tau_C = 1.49\ g_{cat}\ s\ Nl^{-1}$ (□, ■).

evidenced by higher activation energy and lower pre-exponential factor (Table 4). The worsening in $LaMnO_3$ activity by Pt addition may be due to the decrease in the catalyst specific surface caused by the co-presence of the noble metal and perovskite in the γ-alumina pores. The observed results are in accordance with data reported by Giebeler et al. [27] in a recent study on methane oxidation on Pt, Pd, Rh promoted $LaMnO_3$ catalysts. Specifically, unless a pre-reducing treatment is applied, an insignificant role of noble metals in enhancing perovskite activity was traced back to the particular morphology of the mixed phase catalyst in which Pt, Pd and Rh were incorporated in $LaMnO_3$ lattice rather than forming another phase

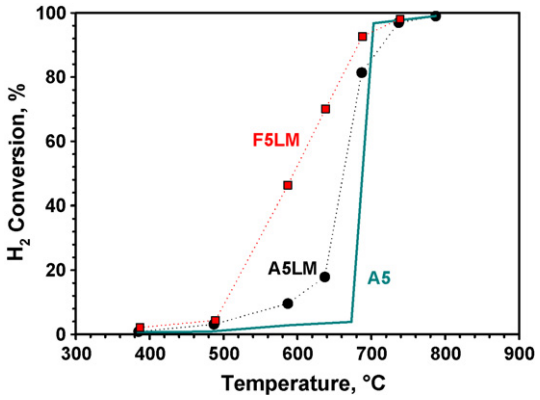

Fig. 6. Hydrogen combustion tests on perovskite and on "catalyst free" α-alumina substrate. F5LM, $\tau_C = 1.44\ g_{cat}\ s\ Nl^{-1}$ (■); A5LM, $\tau_C = 1.71\ g_{cat}\ s\ Nl^{-1}$ (●); A5 (▬).

on the catalyst surface. Moreover, the ineffectiveness of adding Pt to $LaMnO_3$ in enhancing catalytic performances is expected because of the lower activity of the noble metal in methane combustion if compared with that of the perovskite, as shown in Fig. 5. Finally, the following scale of activity is observed in methane combustion: $LaMnO_3$ > Pt–$LaMnO_3$ > Pt.

On the other hand, as shown in Fig. 3b, Pt guarantees higher combustion efficiency in terms of CO production. As a matter of fact, Pt catalyst shows the lowest CO selectivity and also the Pt–$LaMnO_3$ sample presents enhanced carbon dioxide selectivity with respect to the undoped catalyst. These results indicate that platinum-containing catalysts present an higher activity than perovskite itself in the oxidation of CO. Actually, CO is produced in gas phase side reactions activated in the range of relatively low temperature (in comparison with typical temperatures of flame combustion) or via catalytic routes, and subsequently converted to CO_2 by the catalyst itself. Moreover, the lower selectivity to CO shown by F5Pt1 compared to that of F5Pt1LM, characterized by the same amount of platinum, indicates that Pt exhibits lower activity when dispersed on the perovskite matrix compared to alumina, so allowing the occurrence of gas phase oxidation of a larger fraction of methane. This may be due to different dispersion or migration of Pt inside the perovskite structure, effectively reducing the amount of noble metal available for the catalysis.

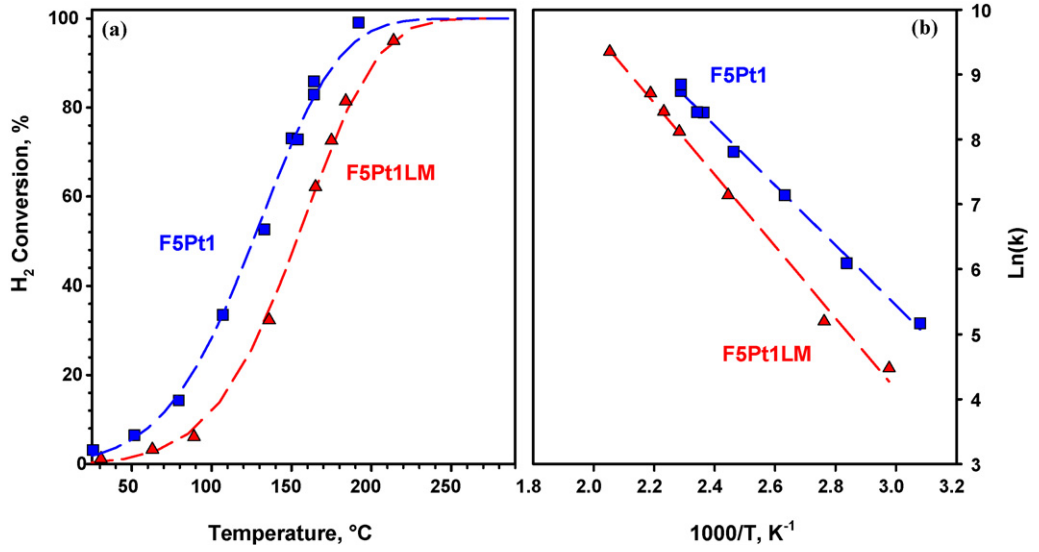

Fig. 7. Hydrogen combustion on different active phase. (a) Fuel conversion as a function of temperature; (b) Arrhenius plot. F5Pt1LM, $\tau_C = 1.53\ g_{cat}\ s\ Nl^{-1}$ (▲); F5Pt1, $\tau_C = 1.49\ g_{cat}\ s\ Nl^{-1}$ (■).

The same catalysts have been also tested in hydrogen combustion. Fig. 6 shows the results of combustion tests carried out on the Pt-free samples (A5LM and F5LM) compared to those performed on A5, while Fig. 7 reports the results obtained over Pt based catalysts.

Perovskite is characterized by a very low activity in hydrogen oxidation, as evidenced by very low conversion up to 500 °C, in agreement with previous studies [28]. Complete H_2 conversion is reached only at about 740 °C in the case of both F5LM and A5LM, with no significant difference between the two samples (F5LM again appears more active at low temperature). Nevertheless, at the specified temperature hydrogen is similarly converted even without a proper catalyst on the α-alumina substrate, A5, probably due to the surface activation of radical reactions proceeding in the gas phase [24,29]. In the case of the catalyst free platelet, actually, at a temperature comprised between 670 and 700 °C a steep increase in hydrogen conversion from 0% to 100% is observed. The presence of a substrate may play a decisive role in the activation of the reactive paths in the gas phase (temperature is still too low for thermal activation to be effective) by promoting the radical formation. However, the overlapping of temperature range of gas phase (surface-assisted) reactions with that of catalytic tests reveals that in the case of H_2 oxidation on perovskite, it is not possible to neglect the contribute of combustion in the homogeneous reactions, the latter being determinant in completing the conversion of the fuel. Such a phenomenon, not ascribed to the presence of a catalyst, is not a classical flame combustion, but is due to the strong reactants dilution that determines a slow flameless process, the so-called "mild combustion" [14,30,31].

On the other hand, promoting perovskite with a little amount of platinum is very effective in enhancing the catalytic activity towards hydrogen combustion (Fig. 7a). As a matter of fact, 10% conversion is attained already at 95 °C; moreover, conversion increases according to a simple Arrhenius law (Fig. 7b) and quite low activation energy (Table 5), indicating the suppression of combustion pathways in the gas phase. An opposite behaviour with respect to methane combustion is detected also comparing performance of F5Pt1LM and F5Pt1, the latter showing the highest activity (Fig. 7a). The higher catalytic activity of F5Pt1 is reflected into an even lower activation energy and an higher kinetic constant calculated at 200 °C (Table 5). As stated before for the activity in the CO oxidation, the lower specific Pt activity in the mixed catalyst may be due to a different dispersion or migration of Pt inside the perovskite structure determining a decrease of the amount of noble metal available for the reaction. Actually, it is very likely, although not investigated in the present work, that the state of Pt in the Pt1LM catalysts is rather heterogeneous. Pt (PtO) micro-clusters are certainly dispersed on the $LaMnO_3/\gamma\text{-}Al_2O_3$ pores, but depending on temperature and reduction degree, a fraction of Pt should enter in the perovkite structure in the manganese position [27].

In Fig. 8 combustion experiments for H_2–CH_4 mixtures performed on F2LM catalyst in a 4 mm high combustion chamber and at total flow rate equal to 40 slph are presented. Specifically, conversion of hydrogen and methane as well as the selectivity to carbon monoxide of converted CH_4 are shown as functions of the temperature in the case of Mix1, Mix2, Mix3, Mix4, Mix7 and Mix8 (see Table 2).

Table 5
Effect of the active phase on H_2 combustion. Resume of some extrapolated experimental data.

Catalyst code	τ_C, g_{cat} s Nl^{-1}	E, Kcal mol^{-1}	k_0, Nl s^{-1} $g_{cat}{}^{-1}$	k (200 °C), mmol s^{-1} $g_{cat}{}^{-1}$
F5LM	1.44	–	–	–
F5Pt1LM	1.53	10.9	2.7×10^5	60.0
F5Pt1	1.49	9.1	6.6×10^4	100.0

Concerning methane conversion (Fig. 8a), in the case of hydrogen free mixture (Mix1), as already reported in Fig. 5, only 40% of fuel is converted at the maximum investigated temperature, due to an insufficient contact time. In Mix2, where 50 vol% of methane is substituted with hydrogen ($H_2/CH_4 = 1$), hydrocarbon conversion does not vary significantly up to 750 °C, despite of the lower inlet methane concentration, so confirming that a first order kinetic law rules the oxidation of CH_4, with acceptable approximation. At the maximum investigated temperature, on the contrary, a steep increase of fuel conversion is observed. This circumstance recurs and it is more pronounced further increasing the H_2/CH_4 ratio in the fuel mixture; in fact, the temperature at which the sudden CH_4 conversion increase occurs becomes lower and lower. It must be underlined that using H_2–CH_4 blends makes possible to completely convert methane at conditions where CH_4 conversion is lower than 50%.

The parallel hydrogen conversion is reported in Fig. 8b. The results obtained on methane-free mixtures (Mix7 and Mix8) resemble those previously reported, with a sudden conversion increase at around 640 °C apparently independent on H_2 concentration, related to the homogeneous ignition. Actually, as we have previously noticed, a Pt-free perovskite catalyst is not significantly active in the oxidation of H_2.

A different behaviour is observed in the hydrogen combustion when H_2–CH_4 fuel mixtures are considered. Comparing H_2 conversion in the case of Mix8 and Mix4, characterized by the same H_2 partial pressure, a significantly lower fuel conversion is detected when methane is co-fed with hydrogen. Specifically, the conversion is the same up to 640 °C while beyond this temperature the "jump" in fuel conversion observed in the case of Mix8 does not occur in the CH_4–H_2 mixture resulting in a lower H_2 conversion in the latter case. Moreover, Mix4 shows a total hydrogen conversion only at about 800 °C while, under the same investigated conditions, 100% conversion was observed at 740 °C for Mix8. The same conclusions are drawn by comparing hydrogen conversion in the case of Mix7 and Mix3, characterized by a lower H_2 content. It is worth noting that, as already observed in the case of pure H_2 combustion, even in the CH_4–H_2 mixture H_2 conversion increases with increasing the fuel inlet partial pressure. In the case of Mix2, characterized by the lowest hydrogen content, the maximum investigated temperature is not enough to guarantee a complete H_2 conversion. In this case it is about 80% where both in Mix3 and Mix4 it was 100%.

On the basis of these results, it is clear that hydrogen shows a promoting effect on methane combustion rate. Such an effect is visible once is reached such a threshold temperature of H_2 ignition in the gas phase and it is more and more significant with increasing the degree of methane substitution with hydrogen. At the same time, the presence of methane in the fuel mixture is unfavourable to hydrogen combustion and, specifically, inhibits the H_2 conversion in the gas phase. A reasonable explanation of such a phenomenon is ascribed to the occurrence of reactive paths in the gas phase involving methane starting from radicals generated by the hydrogen activation. Such an effect of hydrogen on methane occurs because H_2 constitutes a source of radicals at a certain temperature that promotes CH_4 oxidation in the gas phase at relatively low temperature. Moreover, a fraction of these radicals seems to preferentially react with methane, thus resulting no more available to sustain hydrogen combustion and explaining the inhibiting effect of methane on H_2 combustion, according to previous results [18].

A further experimental indication of the occurrence of radical reactions converting methane also in the gas phase can be derived by the analysis of Fig. 6c, where selectivity to carbon monoxide is reported in the case of Mix1, Mix2, Mix3 and Mix4. In the case of hydrogen-free fuel (Mix1), selectivity to CO decreases monotonically with the temperature, as already observed in Fig. 5. In the specific, at the maximum investigated temperature CO selectiv-

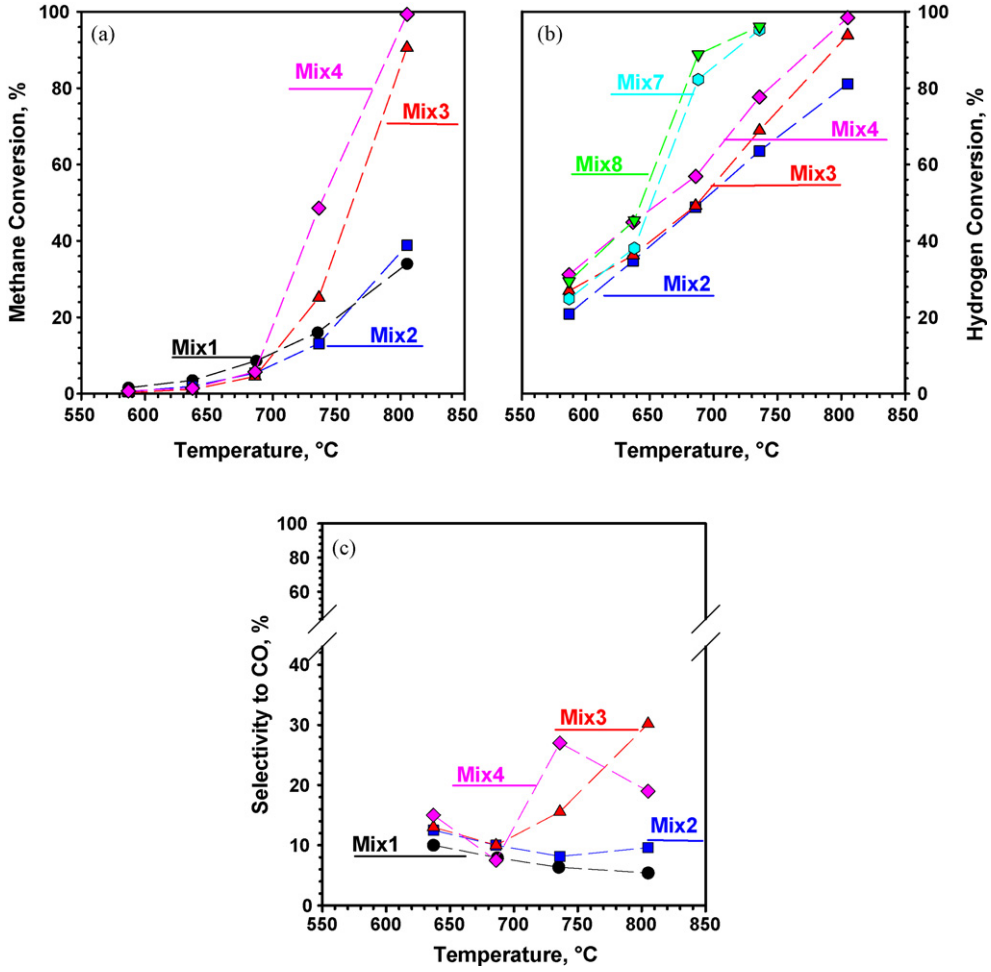

Fig. 8. Combustion of H_2–CH_4 mixtures on F2LM at τ_C = 1.26 gcat s Nl^{-1} and at τ_R = 162 ms (evaluated at STP). (a) H_2 conversion as a function of temperature; (b) CH_4 conversion as a function of temperature; (c) Selectivity to CO as a function of temperature. Mix1 (●); Mix2 (■); Mix3 (▲); Mix4 (◆); Mix7 (●); Mix8 (▼).

ity is about 5%, corresponding to a carbon monoxide production of approximately 50 ppm. In the presence of hydrogen in concentration high enough to allow methane total conversion a different behaviour is observed. For instance, considering Mix3, characterized by an H_2/CH_4 ratio equal to 2, selectivity to CO is very close to that measured for Mix1 up to a temperature of 700 °C, but beyond this temperature and in correspondence with the steep increase observed in methane conversion, CO selectivity strongly increases till to reach much higher values than those detected for Mix1. Moreover, in the case of Mix3, selectivity increases monotonically with temperature beyond 700 °C thus inverting the trend measured for Mix1. In Mix3 selectivity is 30% at about 800 °C, corresponding to a carbon monoxide production of approximately 490 ppm. Similar considerations are valid in the case of combustion experiments of Mix4, up to the complete conversion of methane. The enhanced production of carbon monoxide in correspondence with the increase in methane conversion in H_2–CH_4 fuel shows that hydrocarbon reacts in the gas phase. Actually, hydrocarbon pure catalytic combustion should proceed assuring a quite total selectivity to CO_2. On the contrary, under the investigated conditions, carbon monoxide is a typical product of homogeneous combustion because the temperature is too low to efficiently complete the further CO oxidation to CO_2 [24].

The promoting effect of hydrogen on methane combustion has been also studied by varying the combustion chamber height but maintaining the same flow rate and catalyst amount. In this way, the residence time (τ_R) has been kept variable, while keeping τ_C (contact time) constant. In Fig. 9 methane conversion is reported as a function of the H_2/CH_4 ratio at different values of τ_R. The experiments were carried on F2LM at 40 slpm resulting in a τ_C = 1.26 g_{cat} s Nl^{-1}. The temperature is maintained constant at 800 °C which is high enough to activate the gaseous reactions involving methane. The residence time τ_R corresponding to chamber heights equal to 1, 3 and 4 mm are respectively 11, 34 and 45 ms (evaluated at 800 °C).

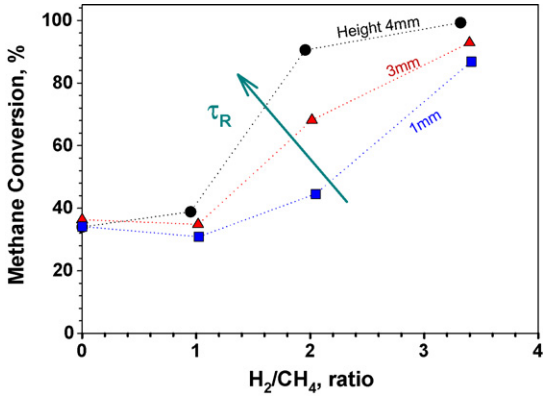

Fig. 9. H_2–CH_4 mixtures combustion on F2LM at τ_C = 1.26 g_{cat} s Nl^{-1} and 800 °C. CH_4 conversion as a function H_2/CH_4 ratio at different values of the residence time (evaluated at 800 °C). τ_R: 45 ms (●); 34 ms (▲); 11 ms (□).

In Fig. 9 methane conversion follows two different trends with varying τ_R depending on H_2/CH_4 ratio. At a H_2/CH_4 ratio less than one, fuel conversion does not depend significantly on the residence time. In these conditions hydrogen is not enough to produce a sufficient amount of radicals that can efficiently attack methane, which is exclusively converted on the catalyst surface and, as a consequence, depends on contact time only.

By increasing the H_2/CH_4 ratio (Fig. 9) in the fuel mixture a significant increase in methane conversion is observed, as reported above, and this enhancement is even improved with increasing the residence time. These results confirm that the promoting effect of hydrogen on methane combustion occurs via homogeneous reactions, whose extent depends on residence time and not on contact time. It must be underlined that the high dilution of the system guarantees isothermal conditions; as a consequence, the enhanced methane reactivity do not depend on thermal effect eventually generated by hydrogen conversion, but is strictly related to a chemical coupling between methane and hydrogen combustion pathways involving the same radicals.

The reported assumptions are supported by several studies devoted to "mild" combustion of CH_4 and/or H_2 [14,30,31], while a completely different behaviour was observed on Pd based catalyst in the H_2-assisted catalytic combustion of CH_4, due to relevant effects of H_2 on Pd reduction and sintering [32]. As it is known, $OH^\bullet$ radicals play the most relevant role in the light-off of methane combustion in the gas phase: these radicals, in fact, chemically activate the hydrocarbon molecules abstracting $H^\bullet$ radicals from them, thus producing $CH_3^\bullet$ (Eq. (3)). As it is shown by Dagaut and Nicolle [14], without co-burning hydrogen, $OH^\bullet$ radicals are mainly produced by the breaking of oxygen molecules through the reaction (Eq. (2)), but due to the high energy bond of oxygen molecule (Eq. (2)) requires high temperature to occur and, specifically, at least 900 °C is needed to have a measurable rate of O_2 dissociation. By adding hydrogen to the methane fuel mixture a changing in the $OH^\bullet$ formation mechanism occurs: in particular, by increasing the hydrogen content in the fuel, hydroxyl radicals are produced more and more significantly through (Eq. (4)) and, specifically, from $HO_2^\bullet$, an intermediate product of low temperature H_2 combustion. More specifically, the presence of hydrogen in the fuel improves system performances in converting methane because determines an increase in the production of hydroxyl radicals at a temperature relatively low thus allowing hydrocarbon combustion in the gas phase at an unexpectedly low thermal level.

$$O_2 + H^\bullet \leftrightarrow OH^\bullet + O^\bullet \quad (2)$$

$$CH_4 + OH\cdot \leftrightarrow CH_3\cdot + H_2O \quad (3)$$

$$H^\bullet + HO_2^\bullet \leftrightarrow OH^\bullet + OH^\bullet \quad (4)$$

Under the investigated conditions, CH_4–H_2 fuel mixtures burn in the gas phase despite of the presence of an active catalyst. On the basis of this result, it is needed to examine in depth the role of the catalyst in future work. However, it is worth noting that the catalyst plays a relevant role on the selectivity of the converted methane: in particular, the detected CO selectivity in the CH_4–H_2 (Fig. 8c) is much lower than expected in a "pure" homogeneous combustion. Based on this consideration, the catalyst, even if it is no more the major responsible of the activation of methane, remains certainly determinant in oxidizing CO to CO_2 improving combustion efficiency.

4. Conclusions

The development of catalytic micro-combustors across the deposition of an active layer on α-Al_2O_3 and FeCralloy slabs gave satisfactorily results. Efficient combustion of H_2 is attained with simple Pt/γ-Al_2O_3 catalyst deposited as a washcoat layer with no problems of gas by-pass nor diffusional resistance, while for methane combustion the most active catalyst investigated is Pt-free and is constituted by the perovskite $LaMnO_3$ dispersed on γ-Al_2O_3. However, the catalyst containing both the noble metal and the mixed metal oxide, Pt–$LaMnO_3$/γ-Al_2O_3, showing intermediate properties, appears as the optimal catalyst for both.

Moreover, methane can be much more efficiently burned if fed with hydrogen. In the presence of H_2, above 700 °C a reaction network involving CH_4 is activated, significantly increasing the methane combustion rate.

References

[1] C. Fernandez-Pello, Micro-power generation using combustion: issues and approaches, Proc. Combust. Inst. 29 (2002) 883–899.
[2] G. Kolb, J. Scürer, D. Tiemann, M. Wichert, R. Zapf, V. Hessel, H. Löwe, Fuel processing in integrated micro-structured heat-exchanger reactors, J. Power Sources 171 (2007) 198–204.
[3] J.A. Federici, D.G. Norton, T. Bruggemann, K.W. Voit, E.D. Wetzel, D.G. Vlachos, Catalytic microcombustors with integrated thermoelectric elements for portable power production, J. Power Sources 161 (2006) 1469–1478.
[4] W.M. Yang, S.K. Chou, C. Shu, Z.W. Li, H. Xue, Development of microthemophotovoltaic system, Appl. Phys. Lett. 81 (2002) 5255–5257.
[5] A. Mehra, X. Zhang, A.A. Ayon, I.A. Waitz, M.A. Schmidt, C.M. Spadaccini, A six-wafer combustion system for a silicon micro gas turbine engine, J. Microelectromech. Syst. 9 (4) (2000) 517–527.
[6] W.M. Yang, S.K. Chou, C. Shu, Z.W. Li, H. Xue, Study of catalytic combustion and its effect on microthermophotovoltaic power generator, J. Phys. D Appl. Phys. 38 (2005) 4252–4255.
[7] X. Wang, J. Zhu, H. Bau, R.J. Gorte, Fabrication of micro-reactors using tape-casting methods, Catal. Lett. 77 (2001) 173–177.
[8] C.M. Spadaccini, X. Zhang, C.P. Cadou, N. Miki, I.A. Waitz, Preliminary development of a hydrocarbon-fueled catalytic micro-combustor, Sens. Actuators A: Phys. 103 (2003) 219–224.
[9] D.G. Norton, D.G. Vlachos, Hydrogen assisted self-ignition of propane/air mixtures in catalytic microburnes, Proc. Combust. Inst. 30 (2005) 2473–2480.
[10] G. Groppi, W. Ibashi, M. Valentini, P. Forzatti, High-temperature combustion of CH_4 over PdO/Al_2O_3: kinetic measurements in a structured annular reactor, Chem. Eng. Sci. 56 (2001) 831–839.
[11] A.K. Datye, J. Bravo, T.R. Nelson, P. Atanasova, M. Lyubovsky, L. Pfefferle, Catalyst microstructure and methane oxidation reactivity during the Pd–PdO transformation on alumina supports, Appl. Catal. A: Gen. 198 (2000) 179–196.
[12] P.O. Thevenin, E. Pocoroba, L.J. Pettersson, H. Karhu, I.J. Vayrynen, S.G. Jaras, Characterization and activity of supported palladium combustion catalysts, J. Catal. 207 (2002) 139–149.
[13] S. Cimino, L. Lisi, R. Pirone, G. Russo, M. Turco, Methane combustion on perovskite-based structured catalysts, Catal. Today 59 (2000) 19–31.
[14] P. Dagaut, A. Nicolle, Experimental and detailed kinetic modelling study of hydrogen-enriched natural gas bled oxidation over extended temperature and equivalence ratio ranges, Proc. Combust. Inst. 30 (2005) 2631–2638.
[15] O. Deutschmann, L.I. Maier, U. Riedel, A.H. Stroemman, R.W. Dibble, Hydrogen assisted catalytic combustion of methane on platinum, Catal. Today 59 (2000) 141–150.
[16] Z. Huang, Y. Zhang, K. Zeng, B. Liu, Q. Wang, D. Jiang, Measurements of laminar burning velocities for natural gas–hydrogen–air mixtures, Combust. Flame 146 (2006) 302–311.
[17] J. Wang, Z. Huang, C. Tang, H. Miao, X. Wang, Numerical study of the effect of hydrogen addition on methane–air mixtures combustion, Int. J. Hydrogen Energy 34 (2) (2009) 1084–1096.
[18] V. Di Sarli, A. Di Benedetto, Laminar burning velocity of hydrogen–methane/air premixed flames, Int. J. Hydrogen Energy 32 (5) (2007) 637–646.
[19] H. Arai, M. Machida, Thermal stabilization of catalyst supports and their application to high-temperature catalytic combustion, Appl. Catal. A: Gen. 138 (1996) 161–176.
[20] http://www.cotronics.com/vo/cotr/pdf/700ins.pdf.
[21] M. Valentini, G. Groppi, C. Cristiani, M. Levi, E. Tronconi, P. Forzatti, The deposition of γ-Al_2O_3 layers on ceramic and metallic supports for the preparation of structured catalysts, Catal. Today 69 (2001) 307–314.
[22] J.G. McCarty, M. Gusman, D.M. Lowe, D.L. Hildenbrand, K.N. Lau, Stability of supported metal and supported metal oxide combustion catalysts, Catal. Today 47 (1999) 5–17.
[23] M.F.M. Zwinkels, O. Haussner, P. Govind Menon, S.G. Jaras, Preparation and characterization of $LaCrO_3$ and Cr_2O_3 methane combustion catalysts supported on $LaAl_{11}O_{18}$- and Al_2O_3-coated monoliths, Catal. Today 47 (1999) 73–82.
[24] S. Cimino, R. Pirone, G. Russo, Thermal stability of perovskite-based monolithic reactors in the catalytic combustion of methane, Ind. Eng. Chem. Res. 40 (2001) 80–85.
[25] R.E. Hayes, S.T. Kolaczkowski, Introduction to Catalytic Combustion, Gordon and Beach Science Publisher, 1997.

[26] R. Byron Bird, W.E. Stewart, E.N. Lightfoot, Transport Phenomena, John Wiley & Sons, New York, 1960.
[27] L. Giebeler, D. Kiebling, G. Wendt, $LaMnO_3$ perovskite supported noble metal. Catalysts for the total oxidation of methane, Chem. Eng. Technol. 30 (2007) 889–894.
[28] S. Cimino, A. Di Benedetto, R. Pirone, G. Russo, CO, H_2 or C_3H_8 assisted catalytic combustion of methane over supported $LaMnO_3$ monoliths, Catal. Today 83 (2003) 33–43.
[29] P. Ciambelli, L. Lisi, R. Pirone, G. Ruoppolo, G. Russo, Comparison of behaviour of rare earth containing catalysts in the oxidative dehydrogenation of ethane, Catal. Today 61 (2000) 317–323.
[30] M. Derudi, A. Villani, R. Rota, Sustainability of mild combustion of hydrogen-containing hybrid fuels, Proc. Combust. Inst. 31 (2007) 3393–3400.
[31] R.W. Schefer, D.M. Wicksall, A.K. Agrawal, Combustion of hydrogen-enriched methane in a lean premixed swirl-stabilized burner, Proc. Combust. Inst. 29 (2002) 843–851.
[32] O. Demoulin, I. Seunier, M. Naveza, C. Poleunis, P. Bertrand, P. Ruiz, Investigation of the physico-chemical implications of the hydrogen presence during H_2-assisted catalytic combustion of methane using Pd(10 wt.%)/γ-Al_2O_3 catalyst, Appl. Catal. A: Gen. 310 (2006) 40–47.